NASA TECHNICAL MEMORANDUM

NASA TM-82399

SUSCEPTIBILITY MEASUREMENTS ON THE SUPERCONDUCTING PROPERTIES OF Nb-Ge ALLOYS

By Thomas J. Rathz
Space Sciences Laboratory

January 1981

NASA

George C. Marshall Space Flight Center
Marshall Space Flight Center, Alabama

MSFC - Form 3190 (Rev June 1971)

TABLE OF CONTENTS

LIST OF ILLUSTRATIONS

LIST OF TABLES

TECHNICAL MEMORANDUM

SUSCEPTIBILITY MEASUREMENTS ON THE SUPERCONDUCTING PROPERTIES OF Nb-Ge ALLOYS

INTRODUCTION

The first observation of superconductivity took place in 1911 when Kamerlingh Onness noticed that the electrical resistance of mercury went to zero upon reaching a critical temperature labeled T_c. A superconductor changes several physical properties upon being cooled to T_c, the most important of which are the loss of all electrical resistance of the material (and the subsequent expulsion of a weak magnetic field) (Meissner effect).

Therein lies the technological importance of superconducting materials for use in electrical transmission lines, motors, generators, and fusion magnets. A large endeavor has been undertaken by many research organizations to produce a material that has superconducting properties at as high a temperature as possible. Table 1 lists some of the more important materials and their associated critical parameters, T_c and H_o. The parameter H_o is the magnitude of the applied magnetic field at $T = 0$ K which will destroy the Meissner effect.

Of all materials studied, the Nb-Ge system is the most technologically promising because of its ability to superconduct well above the boiling point of hydrogen ($T_b = 20.4$ K), which is important for the economical use of superconductors as a practical tool. As seen in Table 1, there are several ways of preparing Nb-Ge in the correct composition, or stoichiometry, that appears to be beneficial for attaining high T_c; this correct composition is Nb_3Ge (β-phase) and must be formed in the correct crystallographic structure (A15).

Sputtered thin films of Nb_3Ge were discovered by Gavaler [1] to have T_c's $\sim$ 22 K; Testardi, Wernick, and Royer [2] immediately verified Gavaler's results, which were subsequently reproduced in films prepared by chemical vapor deposition techniques [3,4].

None of these techniques have been successfully used to make Nb_3Ge in bulk form because of the highly nonequilibrium solidification environment that must exist to form this metastable compound. Rapid solidification by splat cooling has been shown to be one technique of forming these metastable phases [5,6]; however, rapid solidification by undercooling may be a competitive technique [7,8]. Undercooling a material means to lower the temperature of the molten material below the solidus temperature before solidification is initiated.

The most difficult problem in attaining undercooled conditions is the presence of nucleation sites which catalyze solidification. Small molten droplets (5 to 50 μ diameter) dispersed in a carrier fluid [9,10] or droplets free-falling in a containerless environment can reduce these nucleants [7,11,12]. To study undercooling and containerless low-gravity solidification of various Nb-Ge compositions, a drop tube apparatus has been constructed at NASA's Marshall Space Flight Center [7]. This device consists of a 32-m high, 10-cm diameter steel tube which allows 2.6 s of freely falling, containerless, low-gravity cooling of molten droplets in either an inert atmosphere or a 10^{-3} $N \cdot m^{-2}$ (1×10^{-5} torr) vacuum. When Nb-Ge materials are processed in this facility, the superconducting transition temperature will be an important and easily determinable parameter for characterizing the effects of this processing environment.

The objective of this report is to determine the effects on the T_c of bulk Nb-Ge alloys solidified in a containerless low-gravity environment as compared to arc-cast materials. The results of the T_c measurements performed on superconductors processed in the drop tube will be presented, particularly the T_c's of the Nb-Ge materials. Another objective is to describe the electronic system which measured the T_c's and to explain the cause for the observed transitions in terms of the changing susceptibility of the samples. Details of the T_c-measuring apparatus and associated electronics are discussed in this report. The physical significance of the signal itself will be discussed as a possible superconductor characterization technique.

APPARATUS AND TECHNIQUE

At the superconducting transition temperature a perfect type-I superconductor will expel all weak magnetic (Meissner effect) and electrical fields from the sample. By placing a sample in a uniform ac magnetic field and using a surrounding pick-up coil to detect the changing flux density due to the Meissner effect, the T_c can be found to great accuracy. The ac method has the advantages of (1) simplicity of operation, (2) avoidance of introducing strain or impurity by electrical contacts used for resistance-temperature T_c measurements, (3) the same T_c measuring accuracy as resistance and heat capacity measurements [13], and (4)

the capability of measuring the real (pure inductive, χ') and imaginary (pure dissipative, χ'') components of the total system susceptibility, χ, which essentially prevents the sample shape from affecting the transition curves and thereby eliminates a source of T_c error [14].

Analysis of the transition voltage signals in terms of χ' and χ'' was used to obtain superconducting T_c. These material properties can be measured using a temperature-varying method of Fellici [15] which is a technique for measuring the mutual inductance of a set of coils by varying the mutual inductance of a set of opposing coils. The Fellici method has been modified and upgraded by several investigators who were measuring the magnetic susceptibility of materials as a function of temperature. The Hartshorn bridge [15] modification was first used for low temperature measurements by Casimer et al. in 1939 [16] and later by many other scientists interested in low-temperature magnetic properties of materials [17-19].

The coil design used in this work was suggested by M. Strongin of the Brookhaven National Laboratories and consisted of a pair of primaries wound directly on a pair of bucking secondaries. The coil materials were a polyethylene coil form and 36-gauge Formvar-insulated copper wire of 248 and 1800 turns of primary and secondary, respectively (Fig. 1).

With the sample centered inside one of the secondary coils, the calculated magnetic field was homogeneous to within 2 percent over the sample's dimensions. A 1008 Hz primary current of 0.63 ± 0.01 rms mA, stable to 0.01 percent was used, thus providing 11 μT (0.11 G) magnetic field strength. Using the experimental values of Nb-Ge resistivity, the calculated spherical skin depth corresponded to 100 percent penetration [20].

Epoxied inside the coils was a bifilarly wound heater coil connected to a variable current source providing temperature controllability to 1 mK. The sample was inserted up into this arrangement by a polyethylene plug so that a typical 3-mm diameter sphere was centered in the top coil and made contact with a carbon glass resistor (CGR) temperature transducer inserted down into the coil. The copper flange and enclosure provided heat-sinking for the electrical leads and stainless steel support tube as well as evacuability for most of the atmospheric gases and moisture.

The circuit itself was centered about the lock-in amplifier (Fig. 2), the output of which was plotted agains the CGR voltages. Actual CGR values were obtained by readings from a 0.1 μV resolution digital voltmeter (DVM) giving 1 mK resolution below 10 K with an absolute accuracy of ± 20 mK as determined by high-purity Pb and Nb laboratory standards. The field strength and frequency were varied over a suitable range to determine that these were not causing any error in the temperature measurements.

Using a lock-in amplifier provided the measurement of the relative magnetic susceptibility components as a function of temperature because of the phase selectability of the lock-in. The expected real and imaginary components of the signal voltages (ΔV_s) produced by a transitioning superconductor are given as [20]:

$$\mathrm{Re}\left(\Delta V_s^S\right) - \mathrm{Re}\left(\Delta V_s^N\right) = v\omega I_p \left[\ell_1 \cos\theta_1\, \ell_2 \cos\theta_2 \left(\frac{4\pi}{c}\right)^2\right] \chi'' \qquad (1a)$$

$$\mathrm{Im}\left(\Delta V_s^S\right) - \mathrm{Im}\left(\Delta V_s^N\right) = v\omega I_p \left[\ell_1 \cos\theta_1\, \ell_2 \cos\theta_2 \left(\frac{4\pi}{c}\right)^2\right] \left(\frac{\chi^s}{1+\chi^s_N} - \chi'\right) \qquad (1b)$$

where χ^s is the perfect diamagnetic susceptibility value for a particular sample geometry; v is sample volume; ω is frequency; I_p is primary current; ℓ_1, ℓ_2 and θ_1, θ_2 are primary and secondary lengths and coil geometry angles, respectively; c is speed of light. An estimate of the expected transition signal height for Nb was made by using typical parameters and the average conductivity of Nb at 9.30K [21]. From these data it was calculated that the purely inductive voltage change for a transitioning superconductor should be approximately ±101 μV, while the purely lossy component should be approximately -38.5 μV. Typical signal-to-noise ratios at the 101 μV χ' signals were about 4×10^3.

The alloy materials used in this study were obtained from Materials Research Corporation, arc-melted from powders of five-nines (Ge) and four-nines (Nb) purity. Four-nines pure, 0.762-mm diameter Nb wire was also melted in the drop tube for determining processing effects on pure elements which were similar to the actual Nb-Ge alloys and for perfecting melting techniques. A five-nines pure, 1.52-mm diameter Pb shot was used as a T_c reproducibility standard. All samples formed in the drop tube were typically 2- to 5-mm diameter.

DISCUSSION

A. Complex Susceptibility

The relationship between χ' and χ'' and the measured voltages can be explained by the following. If a material is magnetized by an ac magnetic field, $H = H_o e^{j\omega t}$, the magnetization L is generally delayed by a phase angle ϕ because of losses and is thus expressed as $L = L_o e^{j(\omega t - \phi)}$. The total susceptibility is then

$$\chi = \frac{L}{H} = \frac{L_o e^{j(\omega t - \phi)}}{H_o e^{j\omega t}} = \frac{L_o}{H_o} e^{-j\phi} = \chi' - j\chi'' \quad , \tag{2}$$

where

$$\chi' = \frac{L_o}{H_o} \cos \phi, \quad \chi'' = \frac{L_o}{H_o} \sin \phi \quad . \tag{3}$$

χ' expresses the component of L which is in-phase with H so it corresponds to the inductive susceptibility; if there were no losses, we should have $\chi = \chi'$. The component χ'' expresses the lossy part of L which is delayed by the phase angle 90 degrees from H. The measured resultant field is $\vec{B} = \mu \vec{H} + \vec{L}$. For a sphere, Landau and Lifshitz [22] have determined the functional form of the spherical χ' and χ'' components (CGS units):

$$\chi' = - \frac{3}{8\pi} \left[1 - \frac{3}{y} G_- \right]$$

$$\chi'' = - \frac{1}{4\pi} \left(\frac{3}{y} \right)^2 \left[1 - \frac{y}{2} G_+ \right] \tag{4}$$

$$G_\pm = \frac{\sinh (y) \pm \sin (y)}{\cosh (y) - \cos (y)} \quad , \quad y = \frac{2a}{\delta} \quad , \quad \delta = \left(\frac{2}{\sigma \mu \omega} \right)^{1/2} \quad ,$$

where δ is planar skin depth, a is sample radius, σ is conductivity, ω is angular frequency, and μ is the permeability of the materials. For low-strength and low-frequency ac fields, a superconducting sample has $\delta \to 0$, giving $\chi \simeq \chi' = - 3/8\pi$, which is the expected equivalence of a superconducting sphere in a dc field. Figure 3 shows the generalized curves for both components.

The importance of the measurement of both susceptibility components for this study is their ability to answer two questions occurring during any T_c-measuring experiment. The first question relates to the use of χ' in most literature for determining the T_c of a sample. However, much

uncertainty can exist as to the number of phases that may be contributing to so-called "spread-out" transitions that occur over several degrees Kelvin. It is possible to have overlapping transitions of two phases that may be interpreted as being a transition of one phase having compositional, order, or some other type of gradient, and vice versa. The second question deals with the possibility of the superconducting material of the sample consisting of a filamentary structure or flakes that would tend to shield a lower T_c volume and thus give only one transition of much larger signal strength than it actually should be.

Because the susceptibility components are the variables that link the physical properties of the sample to the measured voltage, an understanding of the possible types of superconducting transitions, in terms of the complex susceptibility, that may occur for various types of superconducting materials is necessary before suitable answers can be given for the questions in the previous paragraph. In all cases, as a material becomes superconducting, the inductive component of the susceptibility χ' will always increase monotonically because of the attainment of perfect diamagnetism. However, the resistive, or complex, component of the susceptibility χ'' will be either a sharp change similar to χ' or else have a peak in the curve just prior to a sharp transition. Both of these cases can be seen in Figure 4. The smooth χ'' curve of Figure 4a [23] is easily understood by noting that the purity of the material places the value of χ'' (for $T > T_c$) on Figure 3 well beyond the peak for most typical sized spherical samples. Therefore, as the transition occurs and $\sigma \to 0$, χ'' will not pass through the peak.

These susceptibility characteristics are very evident in the transition of this study's five-nines pure Pb calibration sample shown in Figure 5. In both the χ' and χ'' curves, the T_c is so sharp that it approaches the ideal, discontinuous T_c of a perfect type I superconductor.

A maximum, or peak, in χ'' can be caused by two competing mechanisms [23,24]. As a normal state, multiphased material is cooled in an ac field, high T_c superconducting filaments or flaked inclusions which occupy negligible volume will increase the average current density within the normal material and cause a rise in χ'' by increased dissipation. At slightly lower temperatures, these inclusions may become completely interconnected and eddy-current shielding of the nonsuperconducting phases occurs, causing apparent bulk diamagnetism and a subsequent large decrease in χ''. An example of this mechanism is shown in Figures 4b [23] and 4c [25] and has been metallographically observed by Arrhenius, et al. [26]. If these inclusions were homogeneous volumes such as cylindrical regions (i.e., dendrites), the eddy currents now generated by the transition would be reduced and not cause any increase in the average current density because the volume of metal being penetrated by magnetic flux would be reduced proportionally. However, nonhomogeneous volumes, such as compositional gradients in the dendrites, will cause a broadened and peaked χ'' curve because of the increased or decreased dissipation that will occur as the magnetic flux is expelled into a greater or lesser resistance material for a given change in temperature.

The height of the maximum in χ'' depends strongly on whether the matrix became superconducting during the interval of a filamentary transition. Criteria have been established by Strongin [24] for semi-quantitatively discerning filamentary versus bulk superconducting properties of a sample. These are:

1) If in a superconducting transition the peak of χ'' is a significant fraction of χ', e.g., greater than 10 percent, then it may be assumed that a homogeneous bulk transition is not being observed.

2) If multiple peaks are observed in χ'', it is reasonable to infer that the different peaks correspond to different transitions occurring in different parts of an inhomogeneous specimen. Mention must be made of a differential paramagnetic measurement used by Hein and Falge [27] as another, more quantitative magnetic method of determining bulk versus filamentary transitions.

In the following discussion of the transition curves of this study, only that temperature interval is shown in which the measuring apparatus was sensitive enough to reveal any transitions. Figure 6 shows an intercomparison among the Pb and Nb calibration samples and the empty coil (background) signals. These signals were the purely inductive component (χ') of the induced emf of the bridge unbalance. Since only relative changes in the signal are required, the zero level of the figures was taken arbitrarily as the point at which the temperature measurements began, occurring well within the superconducting state of the sample. The empty coil typically produced about 1 to 2 percent systematic voltage variation above 18 K; also, excellent thermal response (i.e., lack of hysteresis) was obtained.

Concerning the susceptibility measurements made on the Nb-Ge drop tube samples, DT078 and DT095 each exhibited two transitions, as indicated by a nonsharp χ' transition. As seen in Figure 7 for sample DT095, the χ' curve verified the use of χ'' for determining that there were two distinct transition phases.[1] One phase (peaked χ'') was slightly more inhomogeneously composed, strained, etc., than the other phase having no observed filamentary structure. Similarly, Figure 8 shows a typical set of curves obtained on Nb-Ge (18.2 a/o) of original starting material and drop tube-processed sample DT085. In the as-cast material, a double-peaked χ'' trace similar to that of Figure 4c is suggestive of a two-phased transition. Not very obvious in Figure 8a is a slight "kink" in the transition for χ' which would have been the only hint of a possible overlapping of transitions if the χ'' component was not also measured. When the as-cast curves of Figure 8a are compared to the curves of DT085 in Figure 8b, a smoothly varying χ' and a single-peaked χ'' are indicative of one phase becoming superconducting. One possible explanation of the disappearance of the double-peaked χ'' is that homogenization occurred between two phases of slightly different composition after processing in the drop tube environment.

1. The term "phase" is used rather loosely here. A more correct terminology would be "a material with different composition."

The analysis of the complex susceptibility measurements for the remaining samples of Table 3, as related to each sample's properties (such as homogeneity and number of T_c-participating phases), resulted in interpretations similar to those already discussed. Studies are presently being performed (X-ray diffraction, EDAX, metallography, annealing) which will allow a more quantitative interpretation of the susceptibility. None of the samples of Table 3 showed a χ'' maximum that surpassed 10 percent of the height of χ', implying that no higher T_c filamentary shielding of lower T_c bulk material occurred.

B. Critical Temperatures

Table 2 gives the T_c and transition widths (ΔT_c^W) of a Pb laboratory calibration sample and Nb drop tube samples. The T_c was determined from the point where the χ' transition curve had risen to half its height, and ΔT_c^W was determined from 5 percent and 95 percent height points. The Pb sample had an extremely sharp transition ($\Delta T_c^W \simeq 5$mK), the T_c of which was 7.222 K; this is 0.022 K greater than the NBS value listed in Table 1. The average T_c of the Nb drops was 9.23 ± 0.04 K, which was 0.02 K lower than the NBS quoted value of 9.25 ± 0.02 K. The T_c's of the drop tube-processed Nb samples were lower and the transition widths smaller than unprocessed Nb, probably due to the formation of large-grained or single-crystalline Nb when processe [28]. Thus, the difference between the T_c of Pb and Nb reported he.e versus NBS's values implies a materials problem rather than a drift in the temperature sensor calibration.

Five Nb-Ge "as-cast" compositions from which droplets were made consisted of nonannealed 13.5, 18.2, 22.1, 27.1, and 35.1 atomic percent (a/o) Ge in Nb as spectroscopically determined. The Nb-Ge compositions formed various amounts of the different phases as inferred from the Nb-Ge equilibrium phase diagram of Figure 9. To determine the amounts and types of each phase that can be formed at a specific overall composition requires the information given in Table 4. The known T_c of these phases is included so that a comparison can be made to the T_c's obtained in this report. The only reported Nb-Ge phases that should be superconducting for temperatures above 4.2 K are the equilibrium β and the metastable β' phases. It is expected that any α phase formed in the alloys would have T_c below 4.2 K because of the rapid decrease in T_c for low Ge-content solid solutions which contain transition Nb and nontransition Ge [29]; also, there is a lack of literature reporting any significant T_c of the α phase of higher Ge content.

Table 3 lists the transition temperatures of all the Nb-Ge drops studied to date. Most of the drops had one rather sharp, smooth transition, as seen in the values of ΔT_c^W which are comparable to typical ΔT_c^W for the drop tube-processed Nb. These temperature widths were further divided into the amount of temperature spread for the initial occurrence of T_c and the amount for the end of T_c. These are called T_c^+ and T_c^-, respectively, and are useful indicators of the directional trends the transitions have undergone. Two samples appeared to have two transitions as determined by the nonmonotonically changing χ' and double-peaked χ'' curves. Figure 7 shows an example of DT095, which was definitely a sample with two superconducting phases. Both the χ' and the χ'' signals indicated the occurrence of two transitions rather than one "spread-out" transition.

Two drops, DT091 and DT078, had transitions of approximately 9.3K (not shown in Table 3) which were due to a piece of undissolved pendant Nb wire within the sample. This was verified by agreement between the measured signal voltage magnitude of these transitions and the theoretical signal voltage magnitude calculated by knowing the mass of the Nb pendant wire lost to these alloy droplets in the melting process.

The most significant fact of Table 3 is the increase of almost every drop's T_c above the transition temperature (T_c^A) of MRC purchased, as-cast material. The overall average increase in the T_c of the drop tube-processed samples was 0.47 with two samples, DT077 and DT099, surpassing a 1.0 K increase. To fully visualize these increases and to see any cross correlation among samples, Figure 10 plots the highest T_c sample of each composition with its associated as-cast material. What is not evident in Figure 10 is any "spread-out" transition which occurred for Matthias, et al. (Fig. 11b) for their bulk splat-cooled specimens [5]. Matthias et al. report a T_c value for as-cast 29 a/o Ge samples in Figure 11a and over-annealed samples in Figures 11c that is close to the T_c of the 27.1 a/o Ge droplets of this investigation.

One possible explanation follows as to why the compositions less than 27.1 a/o have the increasingly deformed droplet shapes listed in Table 3. Photographs of drops which had the hemispherical ("C") and splattered ("D$^-$") structures are shown in Figure 12. Solidification of the α phase will be the first and fastest to nucleate; therefore, as the overall composition approaches the eutectic point, the lever-rule says that there should be increasing amounts of slower cooling β phase remaining to solidify and, thus, the droplet would be "mushier" when it hits the bottom of the drop tube. The "A" shaped 22.1 a/o drops are exceptions to the case because these were intentionally made of less mass so that complete solidification could occur in the 2.5 s of free-fall cooling time.

The average increase in the T_c of the 13.5 a/o Ge droplets was 0.95 ± 0.25 K; the 18.2 a/o Ge, 0.55 ± 0.06 K; the 22.1 a/o Ge, 0.36 ± 0.45 K; and the 27.1 a/o Ge, 0.045 ± 0.01 K. Although the increase in T_c can seemingly be grouped according to composition, the 22.1 a/o droplets presented some peculiarities. Comparison of the surface structure of two class "A" droplets in Figure 13 shows an apparent grain refinement of DT099 over that of DT097; also, the T_c of DT099 was 0.82 K greater than that of DT097. Grain refinement is usually associated with high solidification rates brought on by greater amounts of undercooling of a material. However, two class "D" drops (DT093 and DT094) which are postulated to have undercooled very much before splattering at the bottom of the drop tube show equal but opposite amounts (0.45 K) of change in their T_c's over that of the as-cast material.

CONCLUSIONS

The T_c measuring technique employed in this study was verified by using pure samples of Pb and Nb. Analysis of their T_c's showed the measurement technique to be very reproducible and accurate both relatively (±3 mK) and absolutely (±20 mK). The T_c's of the Pb and Nb were within ±20 mK of NBS values, which is within the absolute experimental uncertainty of this study.

The measurement of the in-phase and quadrature-phase components of the sample's susceptibility appears to be helpful in two ways. First, the technique can possibly give some insight into the homogeneity of the specimen. Multiple χ"-peaks indicate several distinct superconducting phases or one phase with compositional inhomogeneities; these were usually seen in the as-cast materials. A single peaked χ"-transition occurring in drop tube processed samples seemed to indicate that improved homogenization took place. Secondly, χ" can provide information on the number of phases that are transitioning.

The Nb-Ge drop tube samples had an increase in their T_c values of up to 16 percent over the as-cast, starting materials. The reason that there may be a correlation between the enhancement in T_c and the droplet shapes could be the slower solidification of the β phase in comparison to the α phase.

Two of the samples studied had a splattered structure which probably indicates these samples were greatly undercooled in the drop tube. One of the samples showed an enhancement in T_c, while the other sample showed an equivalent decrease in T_c. By comparison, Savitsky et al. [34] and Matthias et al. [5] claim that any T_c increases seen in their splat-cooled samples were only for Ge concentrations above that of the eutectic.

Since these splattered samples indicate a possibility of large undercooling, infrared detectors have been installed in the drop tube to determine the amount of undercooling. For pure Nb, undercooling corresponded to 525 K [7], an amount also expected for these alloys. Additional samples, not included in this report, are presently being studied that show an increase in T_c of up to 4 K. Other analyses being performed include X-ray diffraction, metallurgy, and annealing studies to determine the physical parameters of the material and to attempt a heat treatment enhancement of the T_c.

REFERENCES

1. Gavaler, J. R.: Appl. Phys. Lett. 23, (1973), p. 480.

2. Testardi, L. R., Wernick, J. H., and Royer, W. A.: Solid State Commun. 15, (1974), p. 1.

3. Tarutani, Y., Kudo, M., and Taguski, S.: Proc. 5th Int. Cryo. Eng. Conf., Kyoto (1974), p. 477.

4. Braginski, A. I., and Roland, G. W.: Appl. Phys. Lett., 25, (1974), p. 762.

5. Matthias, B. T., Geballe, T. H., Willicns, R. H., Corenzwit, E., and Hull, G. W. Jr.: Phys. Rev., 139 (1965), A1501.

6. Kattamis, T. Z. and Mehrabian, R.: J. Vac. Sci. Tech, 11, (1974), p. 1118.

7. Lacy, L. L., Robinson, M. B., and Rathz, T. J.: J. Cryst. Growth, 51, (1981) p. 47.

8. Hirth, J. P.: Met. Trans., 9A, (1978), p. 401.

9. Perepezko, J. H., and Rasmussen, D. H.: Met. Trans., 9A, (1978), p. 1490.

10. Turnbull, D.J.,: J. Chem. Phys., 20, (1952), p. 411.

11. Nelson, L. S., Levine, H. S., ` sner, D. F., Kurzius, S. C.: High Temp. Sci., 2, (1970), p. 343.

12. Cech, R. E., and Turnbull, D.: Trans. AIMI, 206, (1956),p. 124.

13. Soulen, R. J., and Calwell, J. H.: J. Low Temp. Phys., 5, (1971), p. 325.

14. van de Klundert, L. J. M., Gijsbertse, E. A., and van der Marel, L. C.: Physica, 69, (1973), p. 159.

15. Hague, B., and Foard, T. R.: A. C. Bridge Methods (Pitman Press, New York, 1971), p. 422.

16. Casimer, H. B. G., deHass, W. J., deKlerk, D.: Physica, 6. (1939), p. 241.

17. McKim, F. R., and Wolf, W. P.: J. Sci, Instr., 34, (1957), p. 64.

REFERENCES (Concluded)

18. Lepper, R. Wolff, E. G., Mills, G. J.: In 1972 Applied Superconductivity Conference (American Physical Society), Annapolis, Maryland, 1-3 May 1972.

19. Oda, Y., Takenaka, H., Nagano, H., and Nakada, I.: Solid State Comm., 32, (1979), p. 659, 35, (1980), p. 887.

20. Rathz, T. J., Thesis, M. S.: University of Alabama in Huntsville, May 1980.

21. Hall, L. A. NBS Technical Note 365 (U.S. Dept. of Comm.) (1968).

22. Landau, L. D., Lifshitz, E. M.: Electrodynamics of Continuous Media (Pergamon Press, New York, 1960).

23. Maxwell, E., and Strongin, M.: Phys. Rev. Lett., 10, (1963), p. 212.

24. Strongin, M. and Maxwell, E.: Phys. Lett., 6, (1963), p. 49.

25. Strongin, M., Maxwell, E., and Reed, T. B.: Phys. Rev., 154, (1967), p. 424.

26. Arrhenius, G., Fitzgerald, R., Hamilton, D. C., Holm, B. A., Matthias, B. T., Corenzwit, E., Geballe, T. H., Hull, G. W. Jr.: J. Appl. Phys., 35, (1964), p. 3487.

27. Hein, R. A., and Falge, R. L. Jr.: Phys. Rev., 123, (1961), p. 407.

28. Aziz, R. A., Baird, D. C.: Can. J. Phys., 37, (1959), p. 937.

29. Matthias, B. T., Gebelle, T. H., Compton, V. B.: Rev. Mod. Phys., 35, (1963), p. 1.

30. Jorda, J. L., Flukiger, R., Muller, J.: J. Less-Common Met., 62, (1978) p. 25.

31. Testardi, L. R., and Poate, J. M.: Phys. Lett., 64A, (1977), p. 117.

32. Claeson, T., Invarsson, J., Rasmussen, S. E.: J. Appl. Phys., 48, (1977), p. 3998.

33. A.I.P. Handbook, 3rd Ed., 1972.

34. Savitsky, E. M., Saur, E., Raub, C. J., and Jefimov, Y. V.: Z. Metallkde, 68, (1977), p. 128.

TABLE 1. CRITICAL TEMPERATURES AND CRITICAL MAGNETIC FIELDS FOR SOME SUPERCONDUCTING MATERIALS

Material	Preparation	T_c (K)	H_o (T)
Pb	Bulk	7.200*	0.0803
In	Bulk	3.415*	0.0293
Al	Bulk	1.180*	0.0105
Nb	Bulk	9.25*	0.1980
Nb_3Ge	Thin Film	23.2	39.5
	Quenched	17	--
	As-Cast and Annealed	6.9	--
Nb_3Al	As-Cast	17.75	31.0
	Annealed	18.72	32.4
Nb_3Sn	As-Cast	17.8	--
	Annealed	18.05	26.0
Nb_3Ga	Quenched	20.7	35.5
	As-Cast	15.6	--
	Annealed	16.1	--

*Source: NBS

TABLE 2. MEASURED TRANSITION TEMPERATURES OF Nb AND Pb

Sample	Purity (%)	T_c(K)		T_c^W (K)	T_c Error (K)
Pb Calibration	99.999	7.22		0.005	0.01
Nb. DT017	99.99	9.19		0.126	0.02
NB. DT111	99.99	9.24		0.079	0.02
Nb. DT125	99.99	9.27	$(T_c)_{AVG}$ = 9.23 ± 0.04 K	0.044	0.02
Nb. DT031	99.99	9.21		0.033	0.02
NB. DT068	99.99	9.25		0.018	0.02
Nb. unprocessed					
Rod	99.99	9.31		0.109	0.02
Wires	99.99	9.34		0.238	0.02

NBS Values: T_c(Pb) = 7.200 ± 0.002 K, T_c (Nb) = 9.25 ± 0.02 K

TABLE 3. TRANSITION TEMPERATURES (K) OF THE Nb-Ge SAMPLES

Composition (a/o Ge)	Sample	T_c	ΔT_c^W	T_c^+	T_c^-	$T_c - T_c^A$	T_{c_2}	$\Delta T_{c_2}^W$	Shape
13.5	DT077	8.07	0.79	8.50	7.71	1.13			B
	DT078	7.72	0.54	8.04	7.40	0.78	7.39	0.23	B
	As-cast	6.94	0.99	7.56	6.57				
18.2	DT082	7.18	0.16	7.28	7.12	0.65			C
	DT080	7.04	0.37	7.22	6.85	0.51			C&F
	DT081	7.08	0.13	7.15	7.02	0.55			C
	DT086	7.08	0.58	7.56	6.98	0.55			C
	DT085	7.02	0.85	7.76	6.90	0.49			C
	As-cast	6.53	0.37	6.68	6.31				
22.1	DT099	7.29	0.30	7.33	7.03	1.06			A
	DT095	7.09	0.22	7.16	6.94	0.85	6.12	0.05	B
	DT093	5.82	0.47	6.15	5.68	-0.42			D-
	DT097	6.47	0.74	7.05	6.31	0.24			A
	DT094	6.72	0.74	7.17	6.44	0.49			D-
	DT091	6.56	0.55	6.95	6.40	0.32			I&St
	DT096	6.72	0.73	7.07	6.34	0.48			D+
	As-cast	6.24	0.34	6.49	6.15				
27.1	DT090	6.07	0.07	6.12	6.05	0.03			A
	DT083	6.10	0.19	6.25	6.06	0.06			A
	As-cast	6.04	0.13	6.00	5.94				
33.1	As-cast	6.02	0.23	6.07	5.84				

Shape: I = Incomplete Melting; St = Stinger Attached A = Spherical; B = Spherical with Slight Flat Spots; C = Hemispherical;

D-/D+ = Splattered/Shattered. F = Hit Side of Tube

TABLE 4. PHASES AND T_c VALUES OF Nb-Ge SYSTEM

Phase	Average Composition (a/o Ge)	Chemical Formula	T_c (K)	T_c Reference
α	6	Nb + Ge	≤4	29
β	20.5	Equi. Nb_3Ge	6	5,30
β'	25	Meta. Nb_3Ge	23	31
γ	37.5	Nb_5Ge_3	0.46	32
δ	60	$NbGe_2$	1.9	33

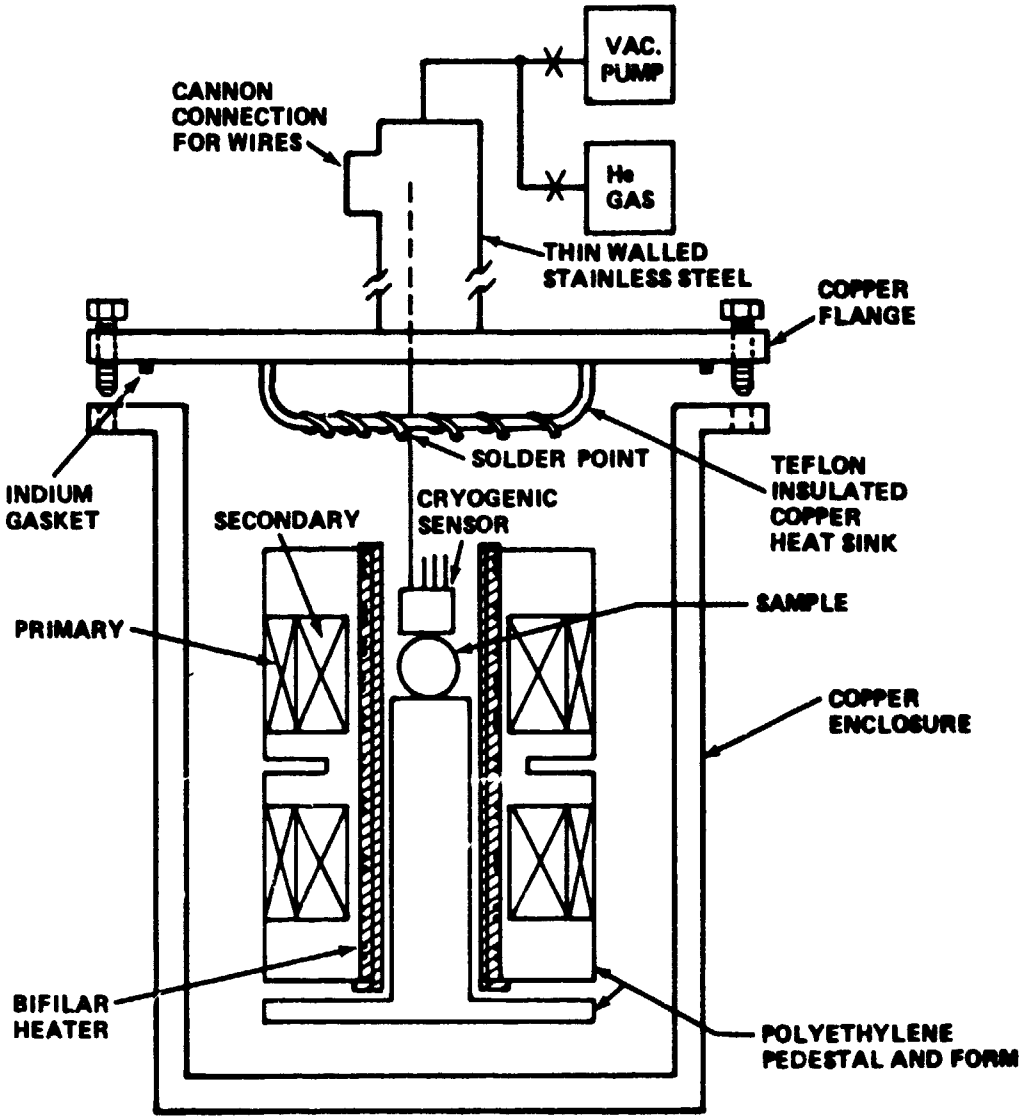

Figure 1. Apparatus for measuring cryogenic magnetic susceptibilities and superconducting transition temperatures of materials.

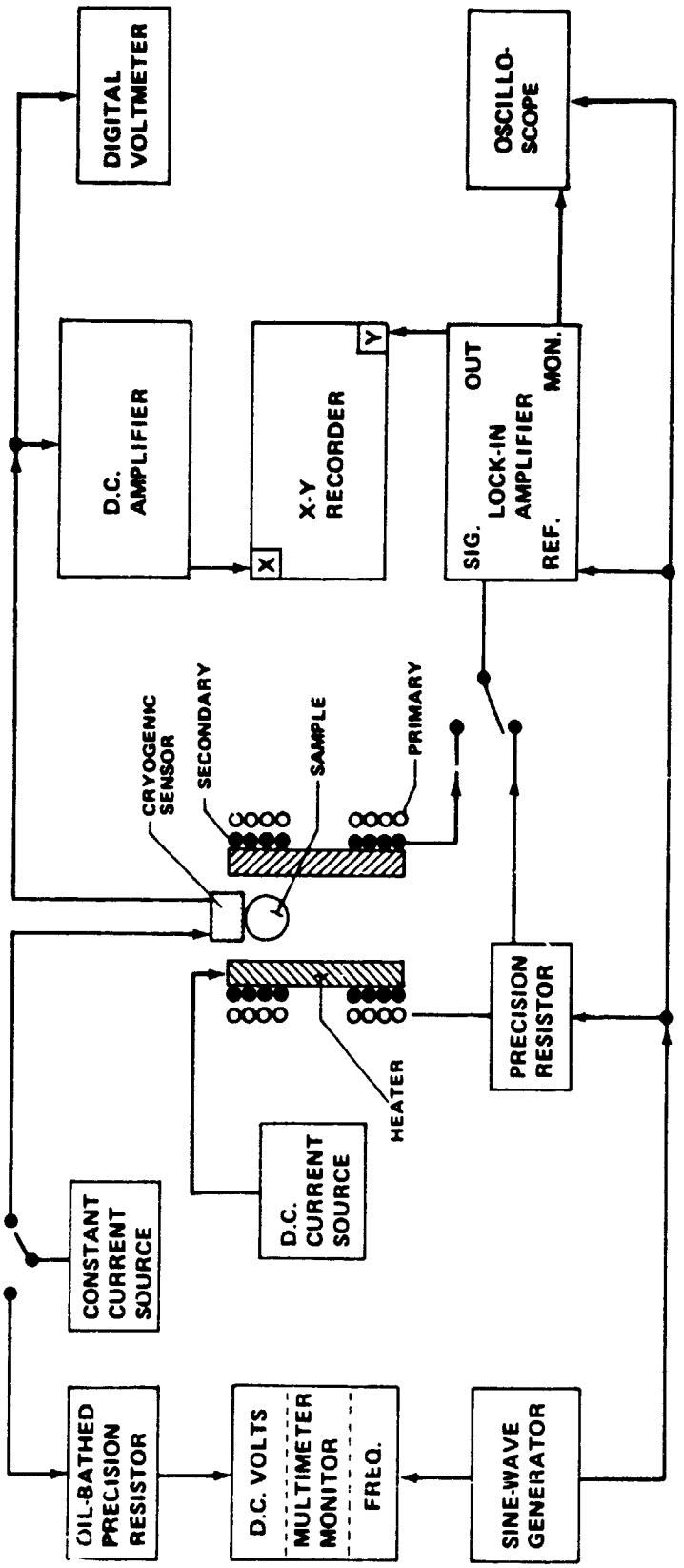

Figure 2. Electronics used to measure cryogenic susceptibilities of materials.

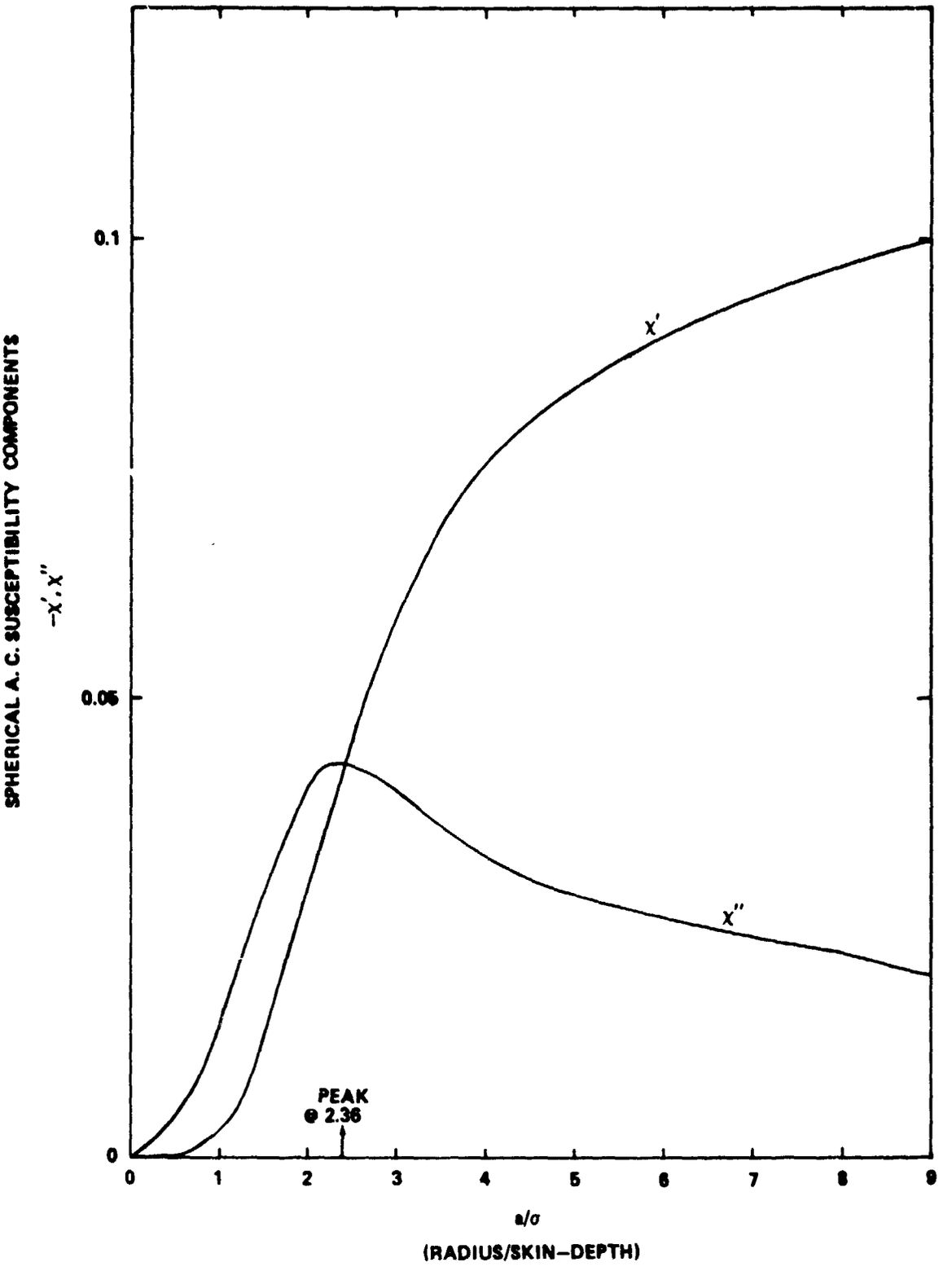

Figure 3. Spherical ac susceptibility components χ' and χ'' versus the radius-to-skin-depth ratio.

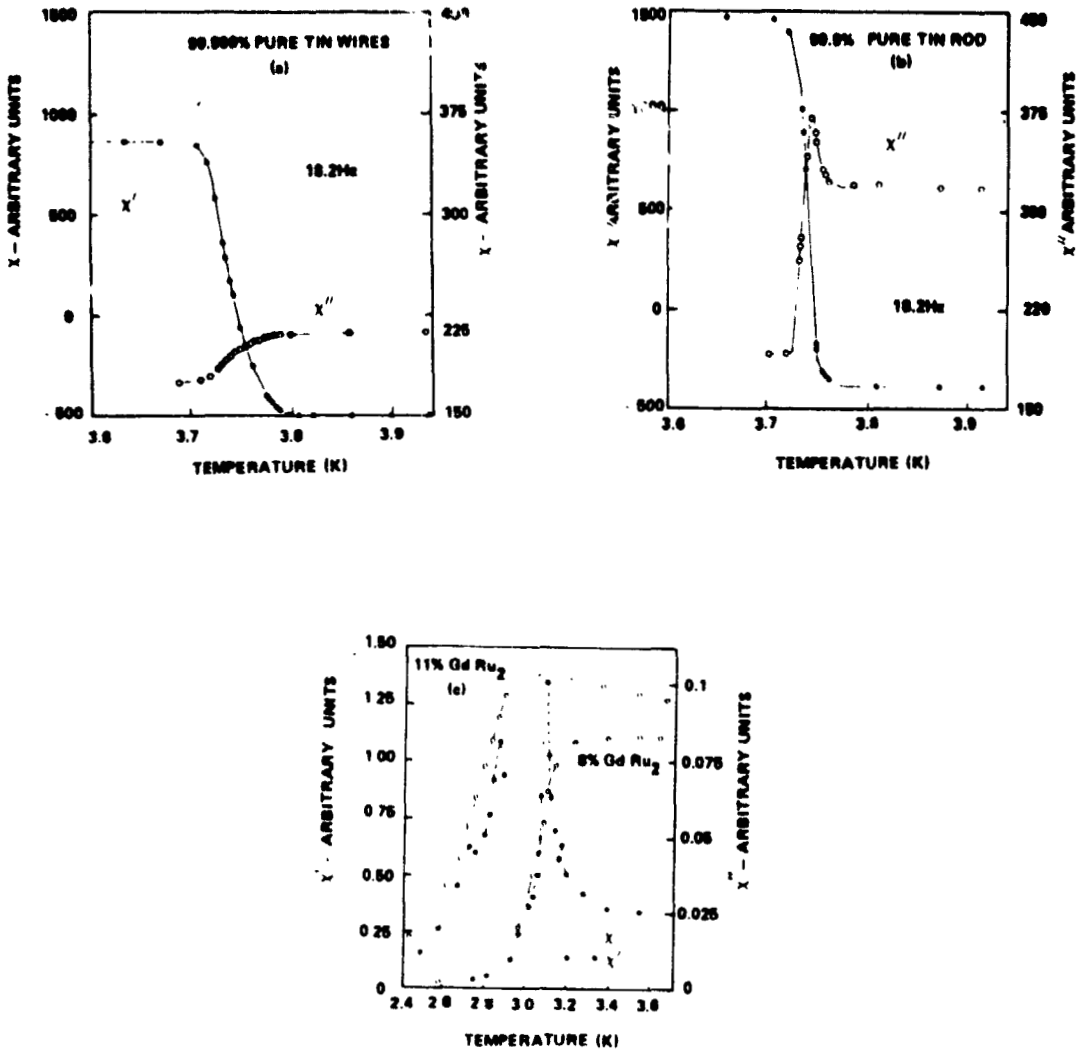

Figure 4. Susceptibility measurements on various materials [23,25].

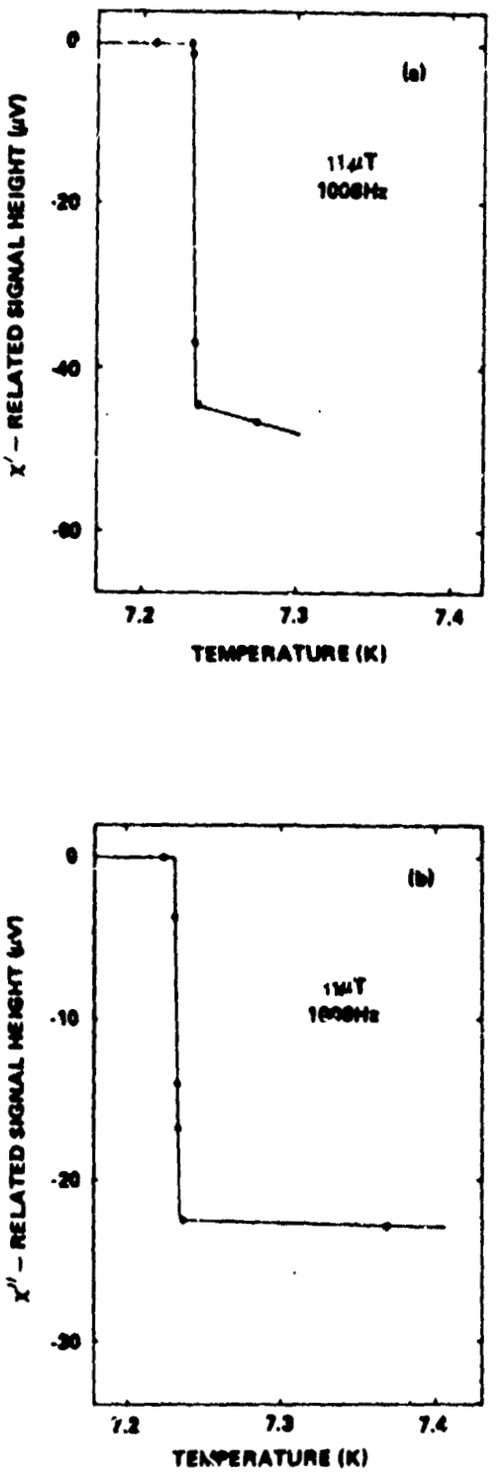

Figure 5. Susceptibility measurements on pure Pb.

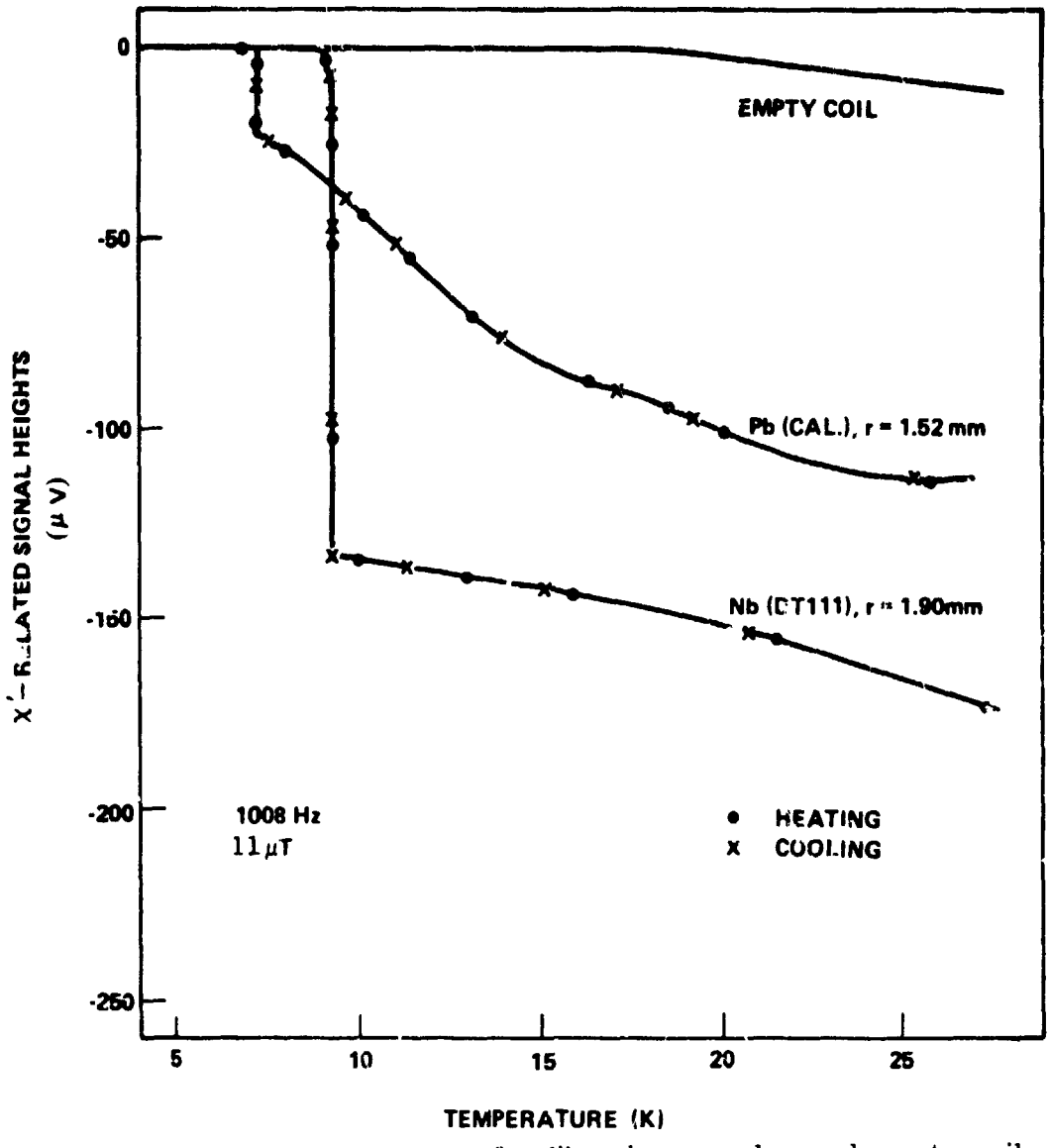

Figure 6. Transition curves of calibration samples and empty coil.

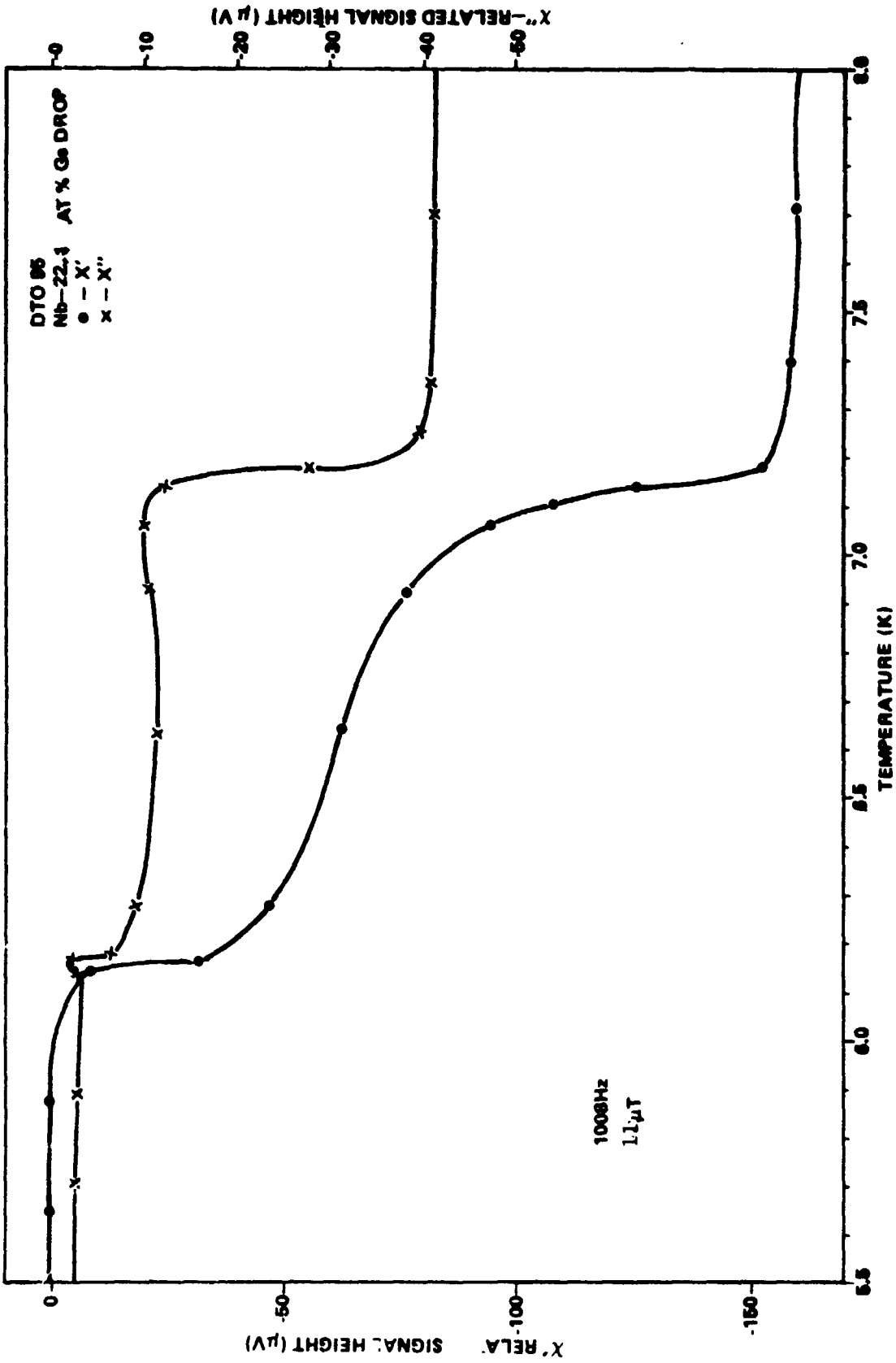

Figure 7. Nb-Ge droplet exhibiting a two-phase transition.

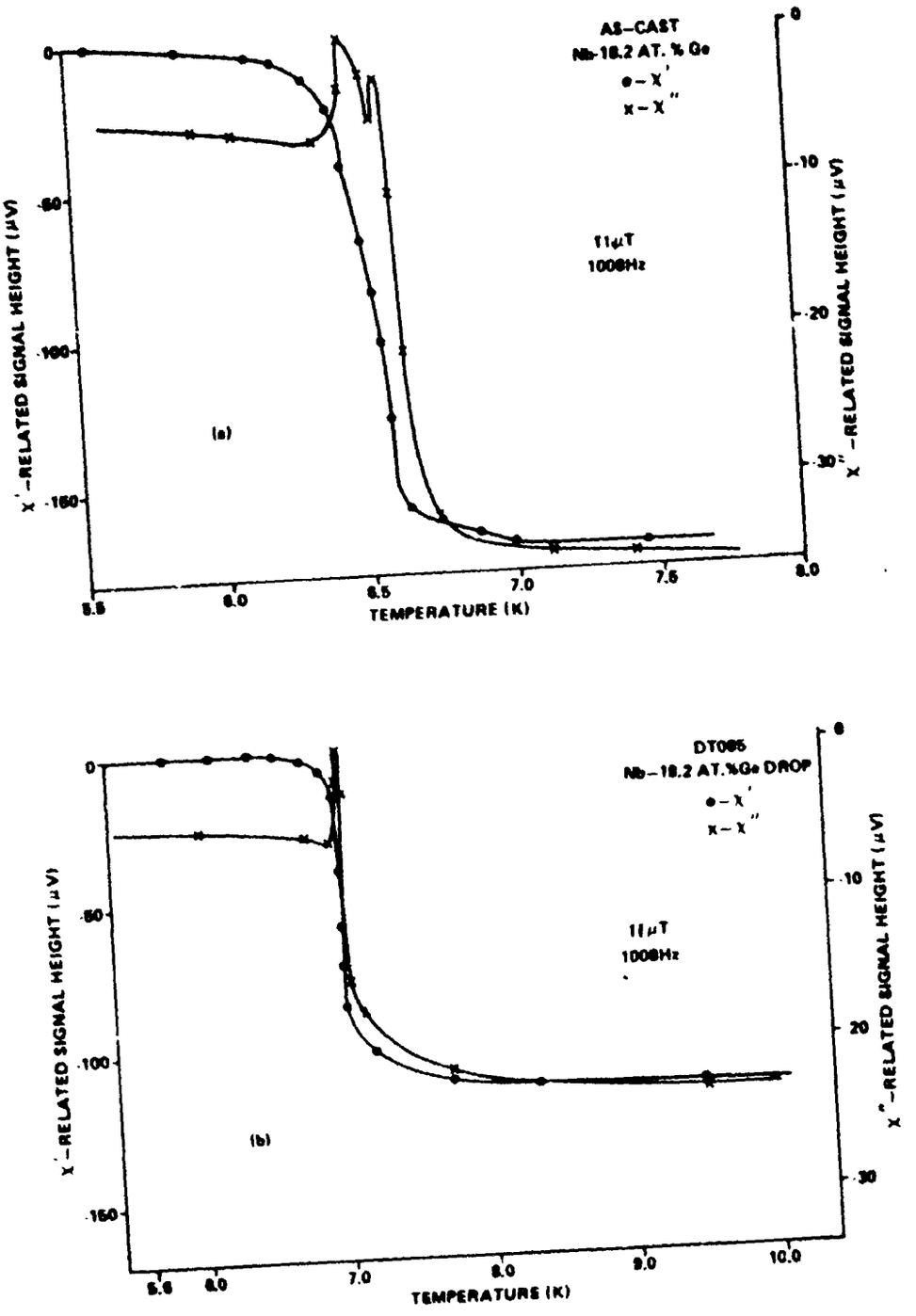

Figure 8. Comparative susceptibility of Nb (18.2 a/o) Ge as-cast and drop tube samples.

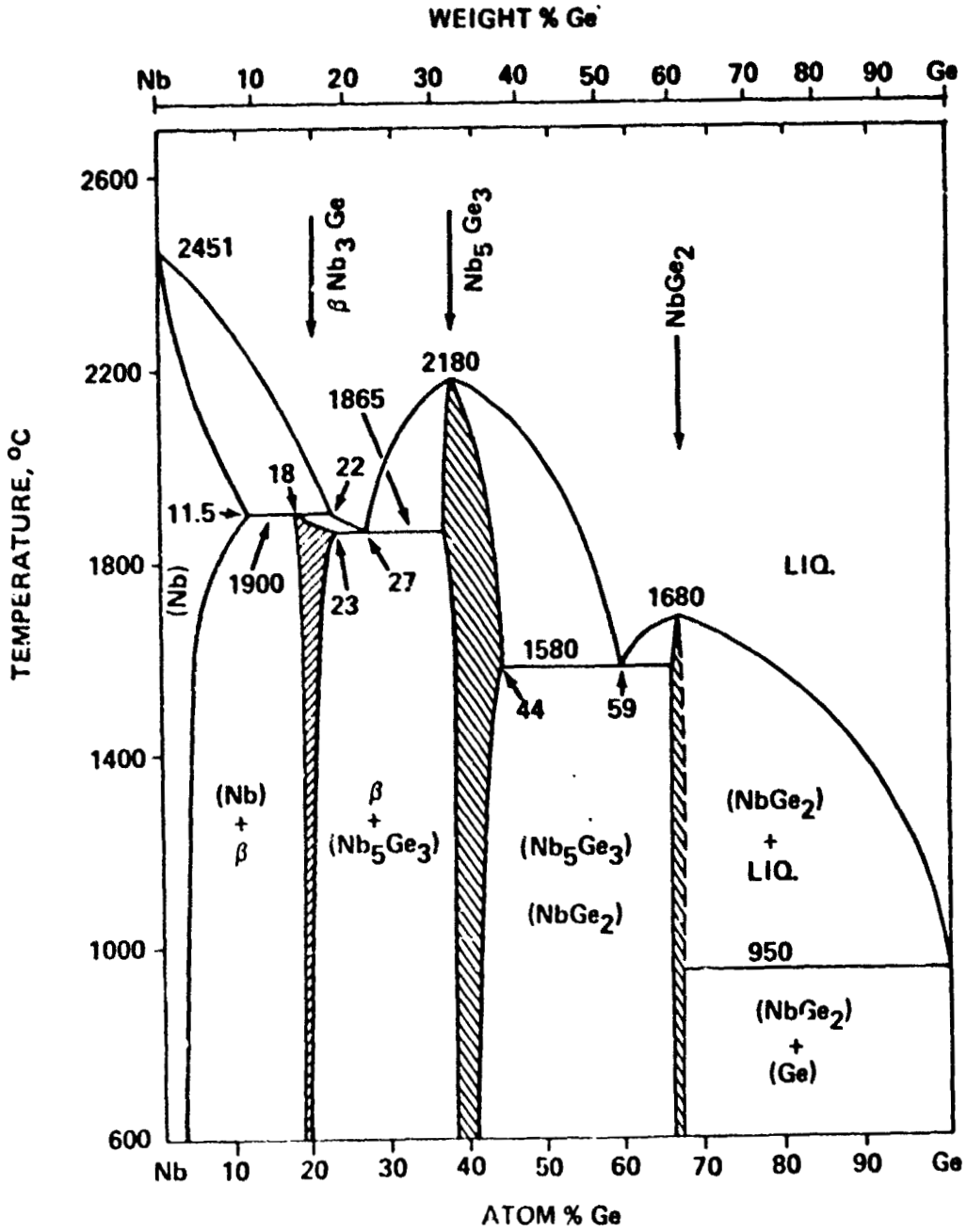

Figure 9. Compositional phase diagram for the Nb-Ge binary [30].

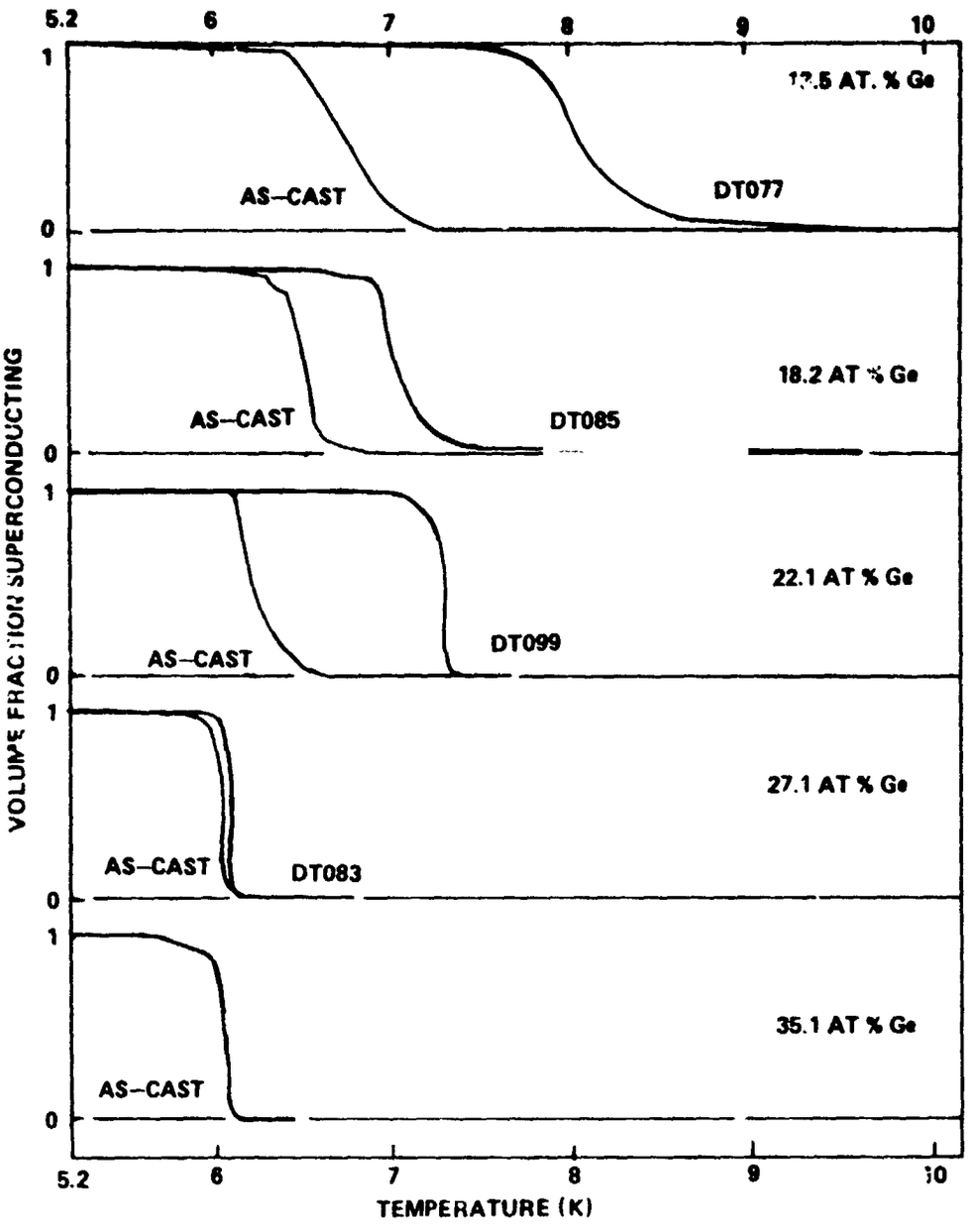

Figure 10. Transition curves of as-cast and drop tube samples of various Nb-Ge compositions.

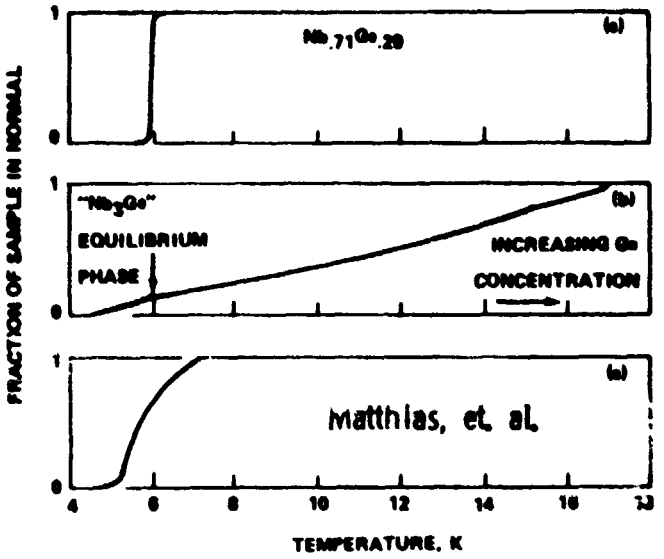

Figure 11. Transition curves for splat-cooled bulk Nb-Ge samples [5]: (a) as-cast, (b) splat-cooled, and (c) over-annealled.

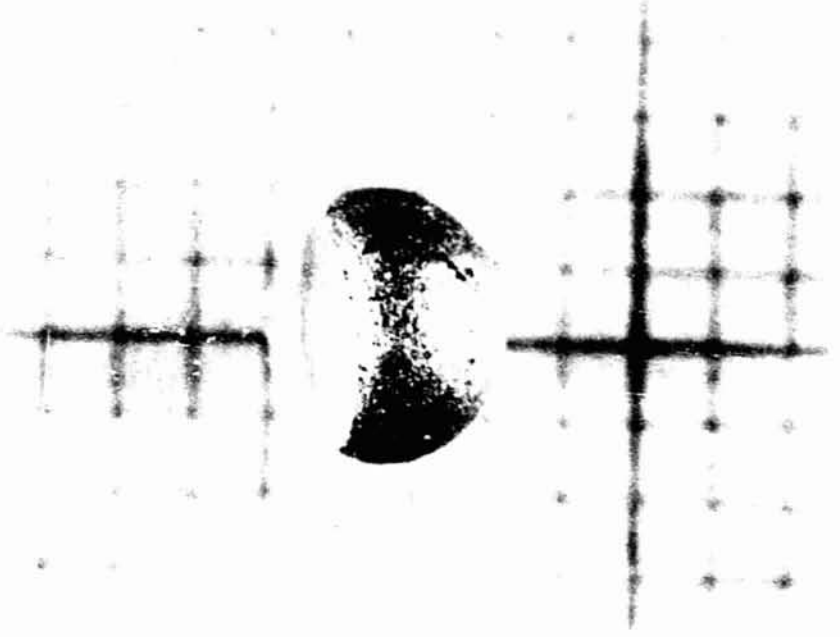

(A) DTO85 Nb – 18.2 a/o Ge 10X

(B) DTO93 Nb – 22.1 a/o Ge 10X

Figure 12. Hemispherical and splattered drop shapes.

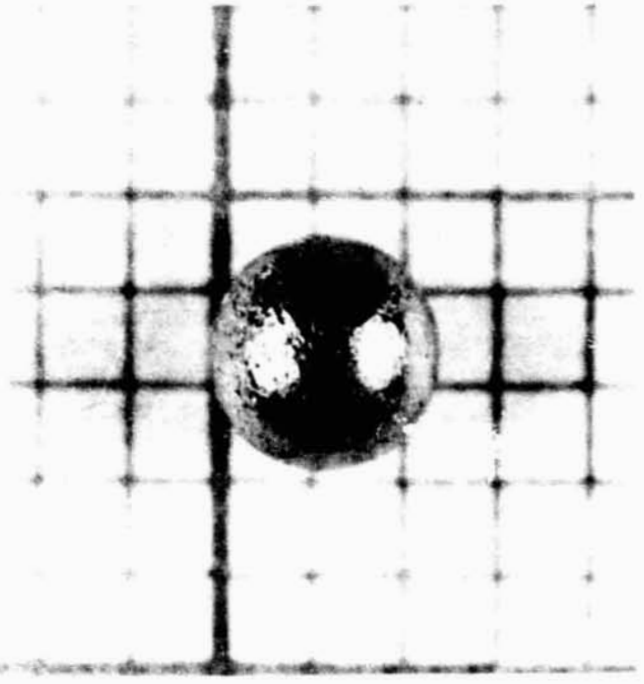

(A) DT097 Nb-22.1 a/o Ge 10X

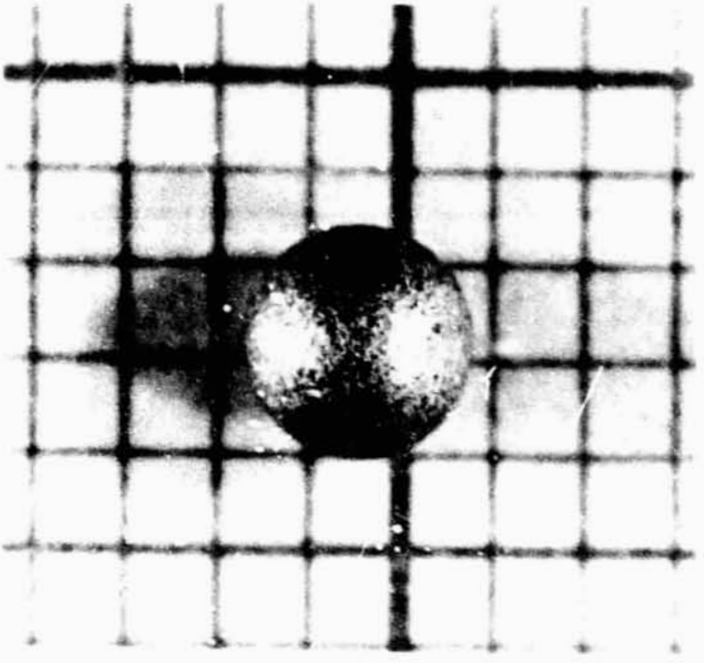

(B) DT099 Nb-22.1 a/o Ge 10X

Figure 13. Two class "A" spherical samples showing differences in surface structure.

APPROVAL

SUSCEPTIBILITY MEASUREMENTS ON THE SUPERCONDUCTING PROPERTIES OF ALLOYS

By Thomas J. Rathz

The information in this report has been reviewed for technical content. Review of any information concerning Department of Defense or nuclear energy activities or programs has been made by the MSFC Security Classification Officer. This report, in its entirety, has been determined to be unclassified

Lewis L. Lacy

LEWIS L. LACY
Chief, Solid State Branch

Robert J. Naumann

ROBERT J. NAUMANN
Chief, Space Processing Division

Charles A. Lundquist

CHARLES A. LUNDQUIST
Director, Space Sciences Laboratory

☆U.S. GOVERNMENT PRINTING OFFICE 1981—740-066/309 REGION NO.4